Inorg. Chem. **1991**, *30*, 3461–3464

hydrolysis awaits further study.

Conclusions

A series of new dicopper(II) and dinickel(II) macrocyclic complexes have been designed as potential mimics of the dinuclear nickel enzyme urease. Their syntheses take advantage of a self-assembly process involving a dinuclear template for Schiff base macrocyclization; in the absence of the appropriate template, no macrocyclized material was formed. The [2 + 2] cyclization to form a tetraimine was found to be highly dependent upon the nature of the bridging ligand. Only imidazolate and acetate were successful with Cu^{II} and Ni^{II}. The failure of other bridging ligands in the synthetic procedure is likely due either to poor ligating ability resulting in too low a concentration of the dinuclear template or to creation of an inappropriate geometry to fit into the cavity of the developing macrocycle. These observations suggest that the method could be extended to other templated macrocyclizations with appropriate choice of the bridging ligand as a function of the cavity size and shape.

Despite the relative ease of formation of complexes **1**–**4**, their solution stability, and indications from the crystal structure of **1** that the macrocycle is quite strain-free, the free ligand L proved to be remarkably sensitive to decomposition in most solvents and in the solid state. One explanation might reside with the dipolar repulsion created in the free ligand upon decomplexation of the metal ions. Macrocycles containing tridentate 2,6-disubstituted pyridines often exist in the uncomplexed form with one of the substituents positioned with its lone pair directed out of the ring to relieve lone-pair repulsions with the pyridine lone pair.[11a,44] In the present case, rotation of the pyridyl–imine C–C bond might be hindered by the rigidity of the *m*-xylyl groups and thus be the source of instability of the free ligand.

The dinuclear complexes displayed spectral features typical of bridging imidazolate and bridging acetate complexes. In the case of **1**, the extent of the magnetic interaction between the two copper(II) centers was correlated to the structural parameters. The study of the magnetic properties of the dinickel bridging complexes is in progress, and their possible relevance to the urease active site would be of great interest.

A comparison of the abilities of the dicopper and dinickel complexes to promote ester hydrolysis indicated that the (μ-acetato)dinickel complex **4** holds some promise for catalytic activity, although the rate enhancement in the case studied is modest. Further refinements to the structure of the dinickel complex, notably investigation of Ni···Ni separations <6 Å, are in progress.

Acknowledgment. We thank M. Bernard and A. Derory for assistance with ESR and magnetic measurements, respectively, and Dr. J. J. André and Dr. P. Legoll for fruitful discussions. The complex $[Co(tterpy)_2](PF_6)_2$ was a gift from Dr. J. P. Collin. This research was supported by a grant from the National Institutes of Health (GM-34841) to C.J.B. and a NATO Collaborative Research Grant to C.J.B. and M.-T.Y. M-T.Y. also thanks the Centre National de la Recherche Scientifique for additional support.

Supplementary Material Available: Tables of atomic coordinates and isotropic thermal parameters, bond lengths, bond angles, anisotropic thermal parameters, and hydrogen atom coordinates (15 pages). Ordering information is given on any current masthead page.

---

(44) Ball, P. W.; Blake, A. B. *J. Chem. Soc.* **1969**, 1415–1422.

(45) Bell, T. W.; Guzzo, F. *J. Chem. Soc., Chem. Commun.* **1986**, 769–771.

Contribution from the Department of Chemistry,
University of Minnesota, Minneapolis, Minnesota 55455

Models for Catechol Dioxygenases. Structure of Bromobis[2-(2′-hydroxyphenyl)benzothiazolato]iron(III) Derived from the Bromoiron(III) Complex of 2,2′-Bis((salicylideneamino)phenyl) Disulfide

Joseph W. Pyrz, Xiangyang Pan, Doyle Britton, and Lawrence Que, Jr.*

Received February 26, 1991

The complex bromobis[2-(2-hydroxyphenyl)benzothiazolato]iron(III), $[Fe(HBT)_2Br]$ or $[Fe(C_{13}H_8NOS)_2Br]$, crystallizes in the orthorhombic space group *Pbcn* (a = 16.30 (1) Å, b = 7.666 (1) Å, c = 22.797 (9) Å, Z = 4). The crystal structure was determined at 24 °C for 2383 out of a total of 4601 reflections with R = 0.051 and R_w = 0.059. The structure reveals a trigonal-bipyramidal complex with the thiazole nitrogens in the axial positions and the phenolate oxygens and the bromide occupying the equatorial sites, structural features that are germane to the active site of the nonheme iron enzyme protocatechuate 3,4-dioxygenase. The title complex derives from an oxidative rearrangement of the bromoiron(III) complex of 2,2′-bis(salicyclideneaminophenyl) disulfide.

The catechol dioxygenases catalyze the oxidative cleavage of catechols as part of nature's mechanism for degrading aromatic molecules.[1] Protocatechuate 3,4-dioxygenase (PCD) is the best characterized of this group;[2] its crystal structure shows an active site consisting of a trigonal-bipyramidal ferric center with an axial and an equatorial tyrosine, an axial and an equatorial histidine, and a solvent molecule in an equatorial site.[3] The structure substantiates many of the active-site features that have been deduced from spectroscopic studies.[4-7] There are no model iron(III) complexes that approximate the crystallographically deduced active site. In the course of our investigations, we explored the coordination chemistry of the pentadentate ligand salpsH_2[8]

---

(1) Stanier, R. Y.; Ingraham, J. L. *J. Biol. Chem.* **1954**, *210*, 799–808. Ornston, L. N.; Stanier, R. Y. *J. Biol. Chem.* **1966**, *241*, 3776–3886.

(2) For a recent review, see: Que, L., Jr. In *Iron Carriers and Iron Proteins*; Loehr, T. M., Ed.; VCH: New York, 1989; pp 467–524.

(3) Ohlendorf, D. H.; Lipscomb, J. D.; Weber, P. C. *Nature* **1988**, *336*, 403–405.

(4) (a) Keyes, W. E.; Loehr, T. M.; Taylor, M. L. *Biochem. Biophys. Res. Commun.* **1978**, *83*, 941–945. (b) Felton, R. H.; Cheung, L. D.; Phillips, R. S.; May, S. W. *Biochem. Biophys. Res. Commun.* **1978**, *95*, 844–850. (c) Que, L., Jr.; Epstein, R. M. *Biochemistry* **1981**, *20*, 2545–2549.

(5) Whittaker, J. W.; Lipscomb, J. D. *J. Biol. Chem.* **1984**, *259*, 4487–4495.

(6) Felton, R. H.; Barrow, W. L.; May, S. W.; Sowell, A. L.; Goel, S.; Bunker, G.; Stern, E. A. *J. Am. Chem. Soc.* **1982**, *104*, 6132–6134.

(7) Pyrz, J. W.; Roe, A. L.; Stern, L. J.; Que, L., Jr. *J. Am. Chem. Soc.* **1985**, *107*, 614–620.

Table I. Crystallographic Data[a] for [Fe(HBT)$_2$Br]·0.5tol

formula	$C_{26}H_{16}BrFeN_2O_2S_2{\cdot}0.5C_7H_8$
fw	634.4
temp, K	297
cryst syst	orthorhombic
space group	*Pbcn*
a, Å	16.30 (1)
b, Å	7.666 (2)
c, Å	22.797 (9)
V, Å^3	6510 (4)
Z	4
D(calc), g cm^{-3}	1.479 (1)
radiation	Mo Kα (λ = 0.71069 Å)
μ, cm^{-1}	20.86
R[b]	0.051
R_w[b]	0.059
GOF[b]	1.59
p[a]	0.05

[a] All calculations were performed by using the Texsan-Texray Structure Analysis Package, Molecular Structure Corp., 1985. The intensity data were processed as described in: *CAD 4 and SDP-PLUS Users's Manual*; B. A. Frenz & Assoc.: College Station, TX, 1982. The net intensity $I = [K(\mathrm{NPI})](C - 2B)$, where K = 20.50 (attenuator factor), NPI = ratio of fastest possible scan rate to scan rate for the measurement, C = total count, and B = total background count. The standard deviation in the net intensity is given by $[\sigma(I)^2 = (k/\mathrm{NPI})^2[C + 4B + (pI)^2]$ where p is a factor used to downweight intense reflections. The observed structure factor amplitude F_o is given by $F_o = (I/Lp)^{1/2}$, where Lp = Lorentz and polarization factors. The $\sigma(I)$'s were converted to the estimated errors in the relative structure factors $\sigma(F_o)$ by $\sigma(F_o) = {}^1/_2[\sigma(I)/I]F_o$. [b] $R = (\sum|(F_o - F_c)|)/(\sum F_o)$; $R_w = \{(\sum w|F_0 - F_c|^2)/(\sum w(F_o)^2)\}^{1/2}$; $\mathrm{GOF} = \{(\sum w(|(F_0 - F_c)|)^2)/(N_{\mathrm{data}} - N_{\mathrm{params}})\}^{1/2}$.

and obtained the complex [Fe(HBT)$_2$Br], which exhibits structural features germane to the PCD active site. We report its structure herein and its relationship to the protein site as well as the interesting chemistry that led to its formation.

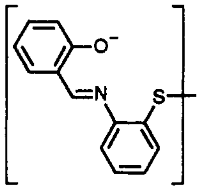

salps^{2-}

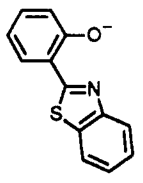

HBT$^-$

Experimental Section

Synthesis. The ligand salpsH$_2$ was synthesized according to the method of Goetz;[9] mp 170–172 °C (lit.[9] 170–172 °C). ^{1}H NMR (δ, ppm, CDCl$_3$): 13.28 (s, –OH, 1 H); 8.98 (s, –CH═N–, 1 H); 8.04 – 7.33 (m, aromatic rings, 8 H). [Fe(salps)Cl] was obtained as black microcrystals from the reaction of FeCl$_3$·6H$_2$O with salpsH$_2$ and 1 equiv of Et$_3$N in hot methanol. Anal. Calcd for $C_{26}H^{18}ClFeN_2O_2S_2$: C, 57.21; H, 3.33; N, 5.13. Found: C, 56.97; H, 3.30; N, 5.11. Vis (CH$_2$Cl$_2$) [λ_{max}, nm (ϵ_M, cm^{-1} M^{-1})]: 514 (sh, 2.59 × 10^3), 562 (2.74 × 10^3). [Fe(salps)Br] was prepared by refluxing a toluene–acetonitrile (1:1 v/v) solution of 1 equiv of salpsH$_2$, 2 equiv of NaOCH$_3$, and 1 equiv of anhydrous FeBr$_3$. The solution was filtered after it was cooled to room temperature. Black microcrystals were induced by adding ether to the filtrate. Vis (CH$_2$Cl$_2$) [λ_{max}, nm (ϵ_M, cm^{-1} M^{-1})]: 510 (2.67 × 10^3), 568 (2.75 × 10^3). Crystals of [Fe(HBT)$_2$Br]·0.5tol (tol = toluene) suitable for single-crystal X-ray diffraction studies were collected from the above filtrate of [Fe(salps)Br] after being stored in the refrigerator for several months. Vis (CH$_2$Cl$_2$) [λ_{max}, nm (ϵ_M cm^{-1} M^{-1})]: 500 (sh, 2.71 × 10^3).

Physical Measurements. Crystallographic data were collected on a crystal (0.7 × 0.3 × 0.2 mm) at the Crystallography Facility of the University of Minnesota Chemistry Department on an Enraf-Nonius CAD4 diffractometer with graphite-monochromated Mo Kα radiation at 297 K using an ω–2θ scan for 0° < θ < 24°. The structure was solved by direct methods using 2383 unique reflections from 4601 total reflections, and crystallographic and refinement data are summarized in Table I. The non-hydrogen atoms were refined anisotropically. Hydrogen atoms were included in the structure factor correlation in idealized positions (d_{C-H} = 0.95 Å), and were assigned isotropic thermal parameters which were 20% greater than the B_{eq} value of the atom to which they were bonded. The standard deviation of an observation of unit weight was 1.59. The weighting scheme was based on counting statistics and included a factor (p = 0.05) to downweight the intense reflections. The maximum and minimum peaks on the final difference Fourier map corresponded to +0.65 and –0.31 e/Å^3, respectively. Neutral-atom scattering factors were taken from Cromer and Waber.[10] All calculations were performed by using the TEXSAN crystallographic software package of the Molecular Structure Corp. The precision of the structure was limited by the presence of a disordered toluene solvate molecule. All bond lengths and selected bond angles are listed in Table II, while the atomic coordinates, thermal factors, and a complete listing of bond angles are available as supplementary material.

Visible spectra were recorded on an HP-8451A diode-array spectrophotometer. NMR spectra were run on an IBM AC300 spectrometer. Elemental analyses were performed on M.H.W. Laboratories (Phoenix, AZ).

Table II. Selected Bond Lengths (Å) and Angles (deg) for [Fe(HBT)$_2$Br][a]

	(a) Bond Lengths		
Fe–Br	2.394 (3)	C1–C2	1.39 (2)
Fe–O1	1.85 (1)	C1–C6	1.42 (2)
Fe–N1	2.157 (8)	C2–C3	1.38 (2)
S1–C6	1.73 (2)	C3–C4	1.36 (2)
S1–C7	1.75 (1)	C4–C5	1.40 (2)
O1–C13	1.31 (2)	C7–C8	1.44 (2)
N1–C7	1.35 (2)	C8–C13	1.41 (2)
N1–C1	1.37 (2)	C9–C10	1.36 (2)
C10–C11	1.40 (2)	C11–C12	1.35 (2)
C12–C13	1.41 (2)		
	(b) Bond Angles		
O1–Fe–O1A	118.9 (7)	N1–Fe–Br	92.0 (3)
O1–Fe–N1	87.2 (6)	N1A–Fe–Br	92.0 (3)
O1–Fe–N1A	90.8 (6)	Fe–O1–C13	135 (1)
O1–Fe–Br	120.6 (3)	O1–C13–C8	124 (2)
O1A–Fe–N1	90.8 (6)	C13–C8–C7	121 (1)
O1A–Fe–N1A	87.2 (6)	C8–C7–N1	128 (1)
O1A–Fe–Br	120.6 (3)	C7–N1–Fe	122 (1)
N1–Fe–N1A	176.0 (5)	C1–N1–Fe	125 (1)

[a] Estimated standard deviations in the least significant digits are given in parentheses.

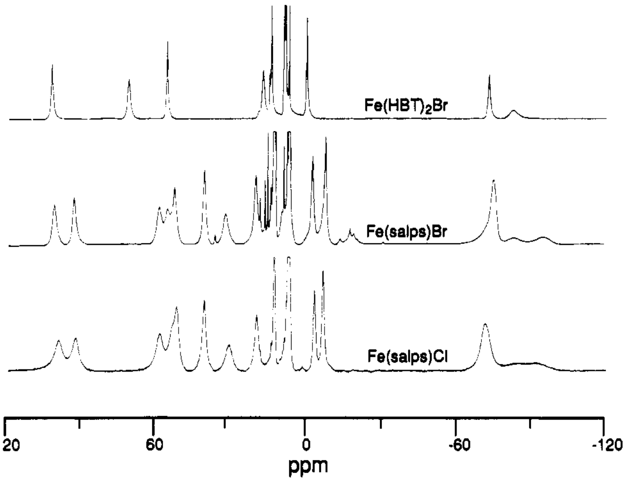

Figure 1. ^{1}H NMR spectra of [Fe(salps)Cl], [Fe(salps)Br], [Fe(HBT)$_2$Br] in CDCl$_3$.

---

(8) Abbreviations used: salpsH$_2$, 2,2′-bis((salicylideneamino)phenyl) disulfide; HBTH, 2-(2′-hydroxyphenyl)benzothiazole; saneH, *N*-(2-phenylethyl)salicylideneamine; salhisH, *N*-[2-(4-imidazolyl)ethyl]-salicylideneamine; TTOPH$_3$ 5-(2-hydroxyphenyl)-10,15,20-tritolylporphyrin; salophH$_2$, 1,2-benzenebis(salicylideneamine); catH$_2$, catechol.

(9) Goetz, F. J. *J. Heterocycl. Chem.* **1967**, *4*, 80–84.

(10) Cromer, D. T.; Waber, J. T. *International Tables for X-ray Crystallography*; Kynoch Press: Birmingham, England, 1974; Vol. IV, Tables 2.2 A and 2.3.1.

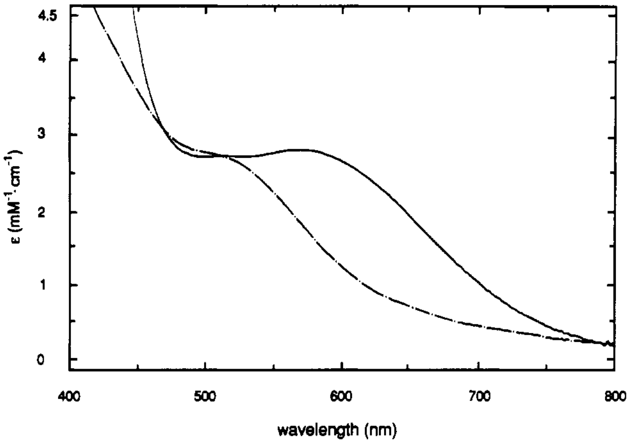

Figure 2. Visible spectra of [Fe(salps)Br] (—) and $[Fe(HBT)_2Br]$ (-·-) in CH_2Cl_2.

Results and Discussion

In the course of our efforts to model the active site of the catechol dioxygenases, we investigated the coordination chemistry of the ligand $salpsH_2$, which is derived from the Schiff base condensation of salicylaldehyde and bis(2-aminophenyl) disulfide. Bertrand and Breece have demonstrated that $salps^{2-}$ acts as a pentadentate ligand in the complex [Fe(salps)Cl], affording a structure with distinct phenolates,[11] i.e.

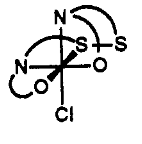

The Fe–O phenolate bond trans to the disulfide is significantly shorter than that trans to the imine. This arrangement gives rise to a visible spectrum showing distinct phenolate-to-iron(III) charge-transfer transitions at 514 and 562 nm, as found for PCD and its inhibitor complexes.[4c] The NMR spectrum of the complex also shows that the low-symmetry structure persists in solution (Figure 1). The two 4-H protons of the phenolates are resolved at 90 ppm, as are the two 3-H protons at −90 ppm.[12] The 0–60 ppm region exhibits a multitude of peaks, also indicating a lack of symmetry in the molecule.

The corresponding Fe(salps)Br complex could be obtained if the complex were precipitated from the reaction solution soon after its formation. This complex exhibits a visible spectrum with maxima at 510 and 568 nm corresponding to the two phenolate-to-iron(III) charge-transfer transitions (Figure 2) and an NMR spectrum strikingly similar to that of the analogous chloride complex (Figure 1).

If, however, the reaction mixture is allowed to stand, dark crystals are obtained that exhibit different visible and NMR spectra. The visible spectrum shows a broad absorption maximum at 500 nm (Figure 2), while the NMR spectrum is indicative of a ligand arrangement with 2-fold symmetry (Figure 1). X-ray diffraction studies demonstrate that [Fe(salps)Br] was transformed into $[Fe(HBT)_2Br]$ upon standing.

$[Fe(HBT)_2Br]$ (Figure 3) crystallizes in the orthorhombic *Pbcn* space group. The iron is in a trigonal-bipyramidal environment with a 2-fold axis through the equatorial Br ligand. The benzothiazoles serve as the axial ligands with Fe–N bonds of 2.157 (8) Å, comparable in length to those found for imidazoles in the six-coordinate $[Fe(salhis)_2]PF_6$ (2.138 (7) and 2.156 (7) Å).[13] The phenolates occupy equatorial positions with Fe–O bonds of 1.85 (1) Å. The Fe–O phenolate bonds are short when compared with those of six-coordinate iron phenolate complexes where the Fe–O bond is typically 1.90–1.92 Å long.[13,14] Comparably short Fe–O bonds are found for the equatorial Fe–O phenolate bonds (1.87 Å) of the other trigonal-bipyramidal Fe^{III}L–phenolate complex, $[Fe(sane)_2Cl]$,[15] and the apical phenolates of the square-pyramidal complexes $Fe_2(TTOP)_2$ (1.85 Å)[16] and Fe(saloph)catH (1.83 Å).[17] Similarly, the equatorial Fe–Br bond (2.394 (3) Å) is comparable in length to those of apical halides in square-pyramidal complexes (2.41 Å).[18] These shorter bond lengths are characteristic of sterically less encumbered sites in five-coordinate complexes.[19]

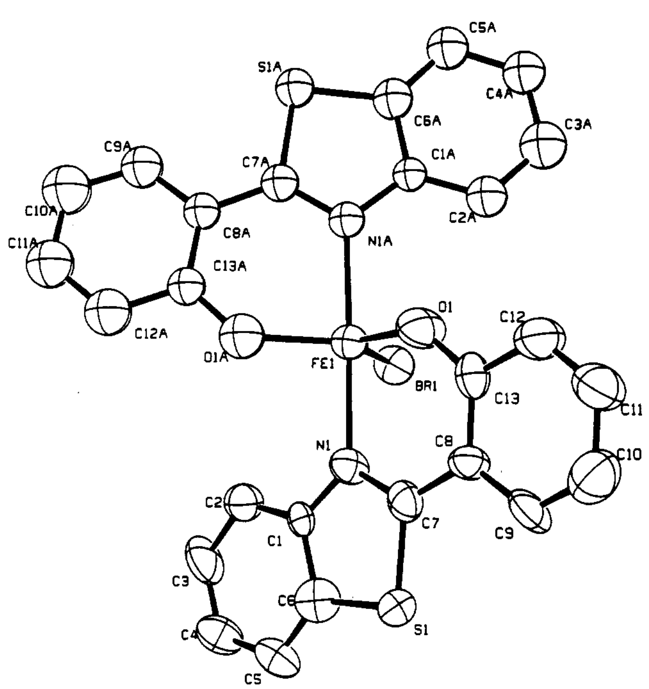

Figure 3. ORTEP plot of $[Fe(HBT)_2Br]$ showing 50% probability ellipsoids. Hydrogen atoms have been omitted for clarity.

The trigonal-bipyramidal coordination sphere represented by $Fe(HBT)_2Br$ with its two phenolate and two thiazole ligands is thus far the closest approximation for the crystallographically determined iron coordination environment in protocatechuate 3,4-dioxygenase.[3] Though the phenolates in the model complex are both equatorial, we can nevertheless use it as a basis for understanding the active site structure of PCD. Recent EXAFS studies on native PCD from *Brevibacterium fuscum* have revealed the presence of a shell of three O/N scatterers at 1.90 Å.[20] On the basis of the equatorial Fe–O(phenolate) distance obtained from $Fe(HBT)_2Br$, the average 1.90 Å distance would thus consist of an equatorial Fe–O(Tyr) bond of ca. 1.85 Å, an axial Fe–O(Tyr) bond of ca. 1.90 Å, and an Fe–O(solvent) bond of ca. 1.95 Å. This range of bond lengths is consistent with the Debye–Waller factor (σ^2) of 0.005 Å² derived from the EXAFS fit. We have thus proposed that the relatively short Fe–O(solvent) distance corresponds to a coordinated hydroxide, a point relevant to the acid–base chemistry of the PCD active site.[20] It is known that substrate

---

(11) Bertrand, J. A.; Breece, J. L. *Inorg. Chim. Acta* **1973**, *8*, 267–272.

(12) NMR spectra are assigned by comparison with other Fe(III)–salicylaldimine complexes, as in ref 7.

(13) Davis, J. C.; Kung, W. S.; Averill, B. A. *Inorg. Chem.* **1986**, *25*, 394–396.

(14) Ainscough, E. W.; Brodie, A. W.; Plowman, J. E.; Brown, K. L.; Addison, A. W.; Gainsford, A. R. *Inorg. Chem.* **1980**, *19*, 3655–3663. Lauffer, R. B.; Heistand, R. H., II; Que, L., Jr. *Inorg. Chem.* **1983**, *22*, 50–55. Yan, S.; Que, L., Jr.; Taylor, L. F.; Anderson, O. P. *J. Am. Chem. Soc.* **1988**, *110*, 5222–5224.

(15) Magurany, C. J.; Strouse, C. E. *Inorg. Chem.* **1982**, *21*, 2348–2350.

(16) Godziela, G. M.; Tilotta, D.; Goff, H. M. *Inorg. Chem.* **1986**, *25*, 2142–2146.

(17) Heistand, R. H., II; Roe, A. L.; Que, L., Jr. *Inorg. Chem.* **1982**, *21*, 676–681.

(18) Decurtins, S.; Shoemaker, C. B.; Wickman, H. H. *Acta Crystallogr.* **1983**, *C39*, 1218–1221. Christidis, P. C.; Rentzeperis, P. J.; Vakoulis, F.; Tsipis, C. A. *Inorg. Chim. Acta* **1984**, *83*, 87–91.

(19) Kepert, D. L. *Inorganic Stereochemistry*; Springer-Verlag: Berlin, 1982, Chapters 4–5.

(20) True, A. E.; Orville, A. M.; Pearce, L. L.; Lipscomb, J. D.; Que, L., Jr. *Biochemistry* **1990**, *29*, 10847–10854.

3464 *Inorg. Chem.* **1991**, *30*, 3464-3476

catechols and inhibitor phenols generally enter the active site as the neutral species, but coordination to the metal center involves the corresponding anion.[21] Some basic species is therefore required to deprotonate the substrate/inhibitor, but the crystal structure indicates the absence of such species save for the coordinated ligands.[3] The coordinated hydroxide easily serves this function.

Last, we comment on the transformation of Fe(salps)Br to $Fe(HBT)_2Br$. This conversion entails an overall two-electron oxidation, consisting of the reductive cleavage of the S–S bond and the oxidative formation of two thiazole rings. While we have no insight into the mechanism of this reaction, it has been demonstrated that there is a tautomeric relationship between 2-(benzylideneamino)thiophenols and 2-arylbenzothiazolines, the latter yielding benzothiazoles upon two-electron oxidation.[9] The reaction we observe is presumably a metal-catalyzed autoxidation.

Acknowledgment. This work was supported by the National Institutes of Health (GM-33162).

Supplementary Material Available: Tables of positional and isotropic thermal parameters, anisotropic thermal factors, and bond angles for $[Fe(HBT)_2Br]\cdot 0.5C_7H_8$ (6 pages); a table of structure factors (6 pages). Ordering information is given on any current masthead page.

---

[21] May, S. W.; Phillips, R. S. *Biochemistry* **1979**, *18*, 5933–5939.

Contribution from the Lehrstuhl für Anorganische Chemie I, Ruhr-Universität, D-4630 Bochum, FRG,
and Anorganisch-Chemisches Institut, Universität Heidelberg, D-6900 Heidelberg, FRG

Coordination Chemistry of Rhenium(V), -(IV), and -(III) with the Macrocyclic Ligands 1,4,7-Triazacyclononane (L) and Its N-Methylated Derivative (L′). Crystal Structures of $[LReCl_3]Cl$, $[L_2Re_2Cl_2(\mu\text{-}Cl)(\mu\text{-}OH)]I_2\cdot 2H_2O$, $[L_2Re_2I_2(\mu\text{-}O)_2]I_2\cdot 2H_2O$, and $[L'_2Re_2Cl_4(\mu\text{-}O)]ZnCl_4$. Effect of π-Donors on the Re–Re Bond Distance

Georg Böhm,[1a] Karl Wieghardt,*,[1a] Bernhard Nuber,[1b] and Johannes Weiss[1b]

Received January 29, 1991

The coordination chemistry of rhenium(III), -(IV), and -(V) with the macrocyclic triamines 1,4,7-triazacyclononane (L, $C_6H_{15}N_3$) and 1,4,7-trimethyl-1,4,7-triazacyclononane (L′, $C_9H_{21}N_3$) has been investigated. Reaction of $[Re^{V}OCl_3(PPh_3)_2]$ with L and ethylene glycol in dry tetrahydrofuran affords monomeric $[LRe^{V}O(O_2C_2H_4)]^+$, which has been isolated in 75% yields as the bromide monohydrate (**1**) or the iodide monohydrate salt. The corresponding reaction with 1,2-dihydroxybenzene and 2-hydroxybenzyl alcohol gives $[LReO(O_2C_6H_4)]Br\cdot H_2O$ (**2**) and $[LReO(O_2C_7H_6)]I$ (**3**), respectively. **1** decomposes at 144 °C cleanly to give quantitatively ethylene and $[LRe^{VII}O_3]I$; **2** and **3** are stable up to 200 °C. **1** was found to be a useful starting material for the synthesis of mononuclear and dinuclear rhenium complexes containing the LRe fragment. Thus reduction of **1** in 1.0 M HCl or HBr with zinc affords $LRe^{III}X_3$ (X = Cl (**5**), Br (**6**)) both of which are oxidized in concentrated CH_3SO_3H in the presence of air to yield $[LRe^{IV}X_3]CH_3SO_3$ (X = Cl (**7**), Br (**8**)). **1** undergoes a series of disproportionation reactions in concentrated hydrohalide solutions. In refluxing 1.0 M HCl, *anti*-$[L_2Re^{IV}{}_2Cl_2(\mu\text{-}O)_2]I_2\cdot 2H_2O$ (**10**), $[L_2Re^{III}{}_2Cl_2(\mu\text{-}OH)(\mu\text{-}Cl)]I_2\cdot 2H_2O$ (**15**), and $[LReO_3]I$ are formed. From HBr and HI solutions of **1**, solid brown materials—presumably $[L_2Re^{IV}{}_2(OH)(H_2O)(\mu\text{-}O)_2]X_3$ (X = Br, I)—were isolated which formed upon heating to 120 °C $[L_2Re^{IV}{}_2X_2(\mu\text{-}O)_2]^{2+}$ (X = Br (**11**), I (**12**)). Oxidation of these brown solids in alkaline aqueous solution with air gives *anti*-$[L_2Re^{V}{}_2O_2(\mu\text{-}O)_2]^{2+}$ (**13**). From an aqueous solution of **13** the neutral complex $[L_2Re_2(OZnCl_3)_2(\mu\text{-}O)_2]$ (**14**) was isolated upon addition of $ZnCl_2$ and NaCl. Reduction of $[L'ReO_3]I$ in 0.5 M HCl with zinc affords the dinuclear complex $[L'_2Re_2Cl_4(\mu\text{-}O)]ZnCl_4$ (**9**). When the reduction is carried out in dry methanol $[L'ReO(OCH_3)_2]PF_6$ (**4**) is formed in ≈5% yield. Compounds **7**, **9**, **12**, and **15** have been characterized by X-ray crystallography. Crystal data: $[LReCl_3]Cl$ (**7**), space group *Pmnn* (No. 58), $a = 7.842$ (4) Å, $b = 12.887$ (7) Å, $c = 12.998$ (9) Å, $V = 1313.58$ Å^3, $Z = 4$; $[L'_2Re_2Cl_4(\mu\text{-}O)]ZnCl_4$ (**9**), space group *Pbnb* (No. 56), $a = 8.614$ (4) Å, $b = 14.589$ (8) Å, $c = 25.24$ (1) Å, $V = 3181.84$ Å^3, $Z = 4$; $[L_2Re_2I_2(\mu\text{-}O)_2]I_2\cdot 2H_2O$ (**12**), space group *Pnmn* (No. 58), $a = 11.941$ (5) Å, $b = 8.410$ (5) Å, $c = 13.828$ (6) Å, $V = 1388.66$ Å^3, $Z = 2$; $[L_2Re_2Cl_2(\mu\text{-}Cl)(\mu\text{-}OH)]I_2\cdot 2H_2O$ (**15**), space group $P\bar{1}$ (No. 2), $a = 8.16$ (1) Å, $b = 8.41$ (1) Å, $c = 9.64$ (1) Å, $\alpha = 84.4$ (1)°, $\beta = 81.3$ (1)°, $\gamma = 82.9$ (1)°, $V = 646.9$ Å^3, $Z = 1$. The dinuclear complexes (edge sharing bioctahedra) **10–15** exhibit multiple metal–metal bonding with Re–Re distances ranging from 2.36 to 2.53 Å depending on the oxidation states of the rhenium centers and π-donor capacity of the terminal ligands. The new compounds have been characterized by UV–vis and NMR spectroscopy; their magnetic and electrochemical properties are also reported.

Introduction

Fusion of two octahedral transition-metal complexes via two μ-oxo bridges leading to an edge-sharing bis(μ-oxo)dimetal species is a very common structural motif in the coordination chemistry of early transition metals in high formal oxidation states.[2] If the metal ion has a d^0 electronic configuration and an oxidation state of +IV, +V or +VI, the metal–metal distance is governed by the $M–O_{oxo}$ bond distances and by a compromise between the electrostatic repulsion between the positively charged metal ions and the negatively charged O^{2-} ions of the bridges. This leads, in general, to metal–metal distances of 2.8–3.2 Å and obtuse M–O–M and acute $O_{oxo}–M–O_{oxo}$ bond angles. Numerous complexes of this type have been crystallographically characterized. If, on the other hand, second- or third-row transition metals with a d^1, d^2, or d^3 electronic configuration are connected in this fashion, the metal–metal distances are usually much shorter (2.4–2.6 Å) and the M–O–M angles are acute whereas the O–M–O angles are obtuse. These structural features have been interpreted as a clear indication for direct metal–metal bonding in such dinuclear species.[3]

Previously, we have reported on the structural chemistry of a series of such complexes containing the dioxo–bis(μ-oxo)dimetal(V) core where the metal is molybdenum(V) and tungsten(V), respectively.[4] Structure A (depicted in Chart I) contains

---

[1] (a) Ruhr-Universität. (b) Universität Heidelberg.

[2] (a) *Comprehensive Coordination Chemistry*; Wilkinson, G., Gillard, R. D., McCleverty, J. A., Eds.; Pergamon Press: Oxford, England, 1987; Vols. III and IV. (b) Holm, R. H. *Chem. Rev.* **1987**, *87*, 1401. (c) Nugent, W. A.; Mayer, J. M. *Metal-Ligand Multiple Bonds*; Wiley: New York, 1988.

[3] (a) Cotton, F. A.; Ucko, D. A. *Inorg. Chim. Acta* **1972**, *6*, 161. (b) Shaik, S.; Hoffmann, R.; Fisel, C. R.; Summerville, R. H. *J. Am. Chem. Soc.* **1980**, *102*, 4555. (c) Cotton, F. A. *Polyhedron* **1987**, *6*, 667.

[4] (a) Wieghardt, K.; Hahn, M.; Swiridoff, W.; Weiss, J. *Angew. Chem., Int. Ed. Engl.* **1983**, *22*, 491. (b) Hahn, M.; Wieghardt, K. *Inorg. Chem.* **1984**, *23*, 3977. (c) Wieghardt, K.; Guttmann, M.; Chaudhuri, P.; Gebert, W.; Young, C.; Enemark, J. H. *Inorg. Chem.* **1985**, *24*, 3151. (d) Schreiber, P.; Wieghardt, K.; Flörke, U.; Haupt, H.-J. *Inorg. Chem.* **1988**, *27*, 2111.

0020-1669/91/1330-3464$02.50/0